

LB/DON/04/03

# Ultrasonic Devulcanization of Sulfur Vulcanized Natural Rubber

17

by

Shantha Maduwage

LIBRARY  
UNIVERSITY OF MORATUWA, SRI LANKA  
MORATUWA

This thesis was submitted to the Department of Chemical and Process Engineering of the University of Moratuwa in partial fulfillment of the requirements for the Degree of Master of Philosophy

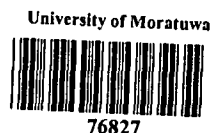
66 "02"  
-----  
678.028.5

TH

Department of Chemical and Process Engineering  
University of Moratuwa  
Sri Lanka

December, 2002

76827



76827

## Declaration

I hereby declare that this submission is my own work and that, to the best of my knowledge and behalf, it contains no material previously published or written by another person nor material which to substantial extent, has been accepted for the award of any other academic qualification of a university or other institute of higher learning except where an acknowledgment is made in the text.



University of Moratuwa, Sri Lanka  
Electronic Theses & Dissertations  
[www.lib.mrt.ac.lk](http://www.lib.mrt.ac.lk)

### *UOM Verified Signature*

Shantha Maduwage  
December, 2002

## Acknowledgements

I am very grateful to my supervisors Dr. A.D.U.S. Amarasinghe and Dr. D.A.I. Munidradasa for their guidance, patience, time, encouragement and commitment throughout the project.

I wish to express my gratitude to the Head of the Department of Chemical and Process Engineering and all other academic staff members for their assistance and encouragement. Special note to mention Dr. K.G.P. Dharmawardana of Department of Electronics Engineering for his guidance in programming Matlab software.

I appreciate the valuable contribution extended to me by Mrs. N. Rathnayake, Director Post Graduate Studies, University of Moratuwa for the completion of the research project. Asian Development Bank helped me to drive this project by way of granting all financial assistance required for the same.



University of Moratuwa, Sri Lanka  
Electronic Theses & Dissertations  
www.lankaalk.com

My special thanks are to Technical and Technical Assistant staff members at Chemical and Process Engineering, and Electronics Engineering departments for their great support for me to carryout experimental works successfully.

Finally, my gratitude must go to my husband, daughter and family for their whole-hearted support for the completion of this thesis.

Shantha Maduwage

December ; 2002



## Abstract

The high-energy ultrasound could be used to devulcanize rubber as it can focus energy into localized sites for selective bond rupture. The research work reported to-date suggests that the ultrasonic technology is more suited to convert rubber waste to a usable material efficiently, effectively and environmental friendly.

The ultrasonic devulcanization reactor consisted of three main sections, namely a power source, ultrasonic transducer with sample holding unit, and a monitoring system to measure the amplitude, frequency and power. N-cyclohexyl-2-benzthiazyl sulfenamide (CBS) accelerated unfilled natural rubber vulcanized with conventional sulfur vulcanizing system and with efficient sulfur vulcanizing system were used as the model rubber compounds in these experiments. 2 mm thick vulcanized rubber sheets were directly kept on the vibrating diaphragm of the ultrasonic transducer. The frequency of ultrasonic wave was varied in a range of 20 to 50 kHz and the power level was varied up to 800 watt. The treatment time was limited to 10 minutes when treated at high power levels. The vibrating amplitudes were measured at different power levels with the variation of ultrasonic frequency.

Curing behaviour, gel content and cross-link density were studied for rubber samples devulcanized at different process conditions. The increase in cross-link density and gel content of the samples treated at lower amplitudes indicated the formation of additional cross-links. However, the higher vibrational energies associated with high amplitudes resulted in lower cross-link densities and gel contents indicating a breakdown of bonds. Cure curves of virgin and devulcanized NR samples suggested that the fast initial curing of devulcanized NR was due to the presence of active sulfidized rubber molecules formed due to break down of some cross-links during devulcanization. The lower maximum torque values observed in the devulcanized samples were due to the partial breakdown of C-C bonds in the main chain. The tensile properties of the revulcanized samples gave comparable results with that of virgin rubber.


A theoretical process model was developed to express the extent of devulcanization in terms of cross-link density. It was based on the vibrational energy transfer mechanism. The model treated the vulcanized rubber as a pure elastic solid containing void regions. Experimental and theoretical values lied within  $\pm 10\%$  error limits. The model showed that the media effect on the nature of void excitation was significant and the viscoelasticity was also considerable. However, the effect due to surface tension was negligible.



# Contents

<b>Chapter 1</b>	<b>Introduction</b>	<b>1</b>
1.1	Devulcanization	1
1.2	Ultrasonic Devulcanization	2
1.3	Theoretical Model for Ultrasonic Devulcanization	3
1.4	Aim and Scope of the Project	4
1.5	Approach	5
1.6	Outline of the Thesis	5
<b>Chapter 2</b>	<b>Literature Review</b>	<b>7</b>
2.1	Disposal of Rubber Waste	7
2.2	Conventional Rubber Recycling Methods	
2.2.1	Chemical Methods	
2.2.1.1	Reclaiming	9
2.2.1.2	Chemical Probes	10
2.2.1.3	Other Chemical Methods	10
2.2.2	Mechanical Methods	12
2.3	Wave energy transfer for rubber reprocessing	
2.3.1	Microwave Devulcanization	14
2.3.2	Ultrasonic Devulcanization	14
2.4	Devulcanization Model	16
2.5	Suitability of present work for selective bond rupture	17
<b>Chapter 3</b>	<b>Reactor for Ultrasonic Devulcanization</b>	<b>20</b>
3.1	Ultrasound	20
3.2	Ultrasonic Transducers	22
3.3	Ultrasonic Reactor	23

<b>Chapter 4</b>	<b>Devulcanization of Accelerated Sulfur Vulcanized Natural rubber</b>	<b>25</b>
4.1	Vulcanization	
4.1.1	Formation of Initial Polysulfidic Cross-links	25
4.1.2	Network Maturing Process	27
4.2	Ultrasonic Devulcanization	31
4.3	Kinetics of Devulcanization	33
<b>Chapter 5</b>	<b>Devulcanization at Low Power Levels</b>	<b>36</b>
5.1	Experimental Techniques	
5.1.1	Compounding Materials	37
5.1.2	Experimental Methods	38
5.2	Characterization methods	
5.2.1	Mooney viscosity	39
5.2.2	Cure Characteristics	40
5.2.3	Gel Content	41
5.2.4	Cross-link density	42
5.2.5	Tensile properties	43
5.3	Vulcanization Experiments	
5.3.1	Mooney Viscosity	45
5.3.2	Cure Characteristics	46
5.3.3	Structural Characteristics	47
5.3.4	Tensile Properties	49
5.3.5	Correlation of Structural properties with Tensile properties	51
5.4	Devulcanization Experiments	
5.4.1	Capacitive Ultrasonic Transducer	54
5.4.2	Inductive Ultrasonic Transducer	57
5.5	Approach to Future Work	
5.5.1	Transducer Performance	61
5.5.2	Methodology Developments	63

<b>Chapter 6</b>	<b>Devulcanization at High Power Levels</b>	<b>65</b>
6.1	Structural Characteristics	
6.1.1	Gel content	
6.1.1.1	CV system	65
6.1.1.2	EV system	68
6.1.1.3	Comparison of Gel Content between CV system and EV system	71
6.1.2	Cross-link density	
6.1.2.1	CV system	73
6.1.2.2	EV system	76
6.1.2.3	Comparison of Cross-link Density between CV system and EV system	79
6.1.3	Relationship between Cross-link density and Gel content	80
6.2	Cure Characteristics	81
6.3	Tensile Properties	84
6.4	Conclusion	86
	 University of Moratuwa, Sri Lanka Electronic Theses & Dissertations www.lib.mrt.ac.lk	
<b>Chapter 7</b>	<b>Process Model for Ultrasonic Devulcanization</b>	<b>88</b>
7.1	Theoretical Modeling	
7.1.1	Devulcanization Model	89
7.1.2	Vibrational Energy Transfer Model	95
7.1.2.1	Acoustic Pressure Amplitude and Void Fraction	98
7.1.2.2	Vibrational Energy Transfer in an Elastic Medium	99
7.2	Simulation of the Model	
7.2.1	Acoustic Pressure Amplitude	101
7.2.2	Void radii at Critical Events	104
7.2.3	Cross-link Density	112
7.3	Comparison of Theoretical and Experiment Results	120



<b>Chapter 8</b>	<b>Effect of Viscoelasticity on Dynamics of Vibrational Energy Transfer</b>	<b>124</b>
8.1	Vibrational Energy Transfer in a Viscoelastic Medium	124
8.2	Viscoelastic Models	127
8.3	Comparison of Elastic Model with Viscoelastic Models	131
<b>Chapter 9</b>	<b>Conclusions and Recommendations for Future Work</b>	<b>139</b>
9.1	Conclusions	139
9.2	Recommendations for Future Work	142
References		
Appendix – I		
Appendix – II		
Appendix – III		
Appendix – IV		
Appendix – V		
Appendix - VI		



## List of Tables and Figures

### Chapter 3

Figure 3.1 Two types of wave motions

Figure 3.2 Ultrasonic Power Source

### Chapter 4

Figure 4.1 Different positions that sulfur attack on the polyisoprene backbone

Figure 4.2 Desulfuration and decomposition of sulfidic cross-links

Figure 4.3 The probable course of sulfur vulcanization of NR in the presence of accelerators and activators

Figure 4.4 Typical chemical groupings present in a sulfur-vulcanized NR network

Figure 4.5 Energy levels of different states of atoms

### Chapter 5

Table 5.1  University of Moratuwa, Sri Lanka  
Electronic Theses & Dissertations  
Dry Formulations for Rubber Compounding

Figure 5.1 Dumb-bell test specimens

Figure 5.2 Mooney viscosity of NR with CV system and EV system

Figure 5.3 Cure curves of CV system and EV system

Figure 5.4 Variation of Gel content with Vulcanizing time for CV system and EV system

Figure 5.5 Variation of Cross-link densities with Vulcanizing time for CV system and EV system

Figure. 5.6 Variation of Tensile properties with Vulcanizing time for CV system and EV system (a) % Elongation at break (b) Tensile strength (c) Modulus@300%elongation

Figure 5.7 Variation of Cross-link density with % Gel content for CV system and EV system

- Figure 5.8 Variation of Tensile properties with Cross-link density for CV system and EV system (a) % Elongation at break (b) Tensile strength (c) Modulus @300% elongation
- Figure 5.9 Variation of Cross-link density with Treatment time for CV system at different power levels,  $f=20$  kHz
- Figure 5.10 Variation of %Gel content with Treatment time for CV system at different power levels,  $f=20$  kHz
- Figure 5.11 Variation of Cross-link density with Treatment time for CV system at different frequencies,  $P=25$  W
- Figure 5.12 Variation of Cross-link density with Supplied power for CV system, at treatment times of 30 and 60 minutes,  $f=20$  kHz
- Figure 5.13 Variation of Cross-link density with Ultrasonic frequency for CV system at constant power levels,  $t=30$  minutes
- Figure 5.14 Variation of %Gel content with Ultrasonic frequency for CV system at constant power levels,  $t=30$  minutes
- Figure 5.15 Variation of Tensile properties with Ultrasonic frequency for revulcanized CV system at constant power levels,  $t=30$  minutes (a) tensile strength (b) modulus @300% elongation
- Figure 5.16 Experimental set up to measure vibrating amplitude
- Figure 5.17 Variation of Vibrating amplitude (peak to peak amplitude) with Ultrasonic frequency at constant power levels

## Chapter 6

- Figure 6.1 Variation of % Gel content of devulcanized CV system with ultrasonic frequency at constant power levels,  $t=10$  minutes (a) power levels up to 500W (b) power levels of 700 W and 800 W
- Figure 6.2 Variation of % Gel content of devulcanized CV system with treatment time at frequencies of 30, 35 and 40 kHz,  $P=800$  W
- Figure 6.3 Variation of % Gel content of devulcanized CV system with vibrating amplitude at constant frequencies,  $t=10$  minutes
- Figure 6.4 Variation of % Gel content of devulcanized and revulcanized CV system with vibrating amplitude,  $f=35$  kHz,  $t=10$  minutes

- Figure 6.5 Variation of % Gel content of devulcanized EV system with ultrasonic frequency at constant power levels (a) 50 W to 200 W (b) 300 W to 800 W,  $t=10$  minutes
- Figure 6.6 Variation of % Gel content of devulcanized EV system with treatment time at frequencies of 30, 35 and 40 kHz,  $P=800$ W
- Figure 6.7 Variation of % Gel content of devulcanized EV system with vibrating amplitude at constant ultrasonic frequencies,  $t=10$  minutes
- Figure 6.8 Variation of % Gel content of devulcanized and revulcanized EV system with vibrating amplitude,  $f=35$  kHz,  $t=10$  minutes
- Figure 6.9 Variation of % Gel content with vibrating amplitude for devulcanized CV system and EV system,  $f=35$  kHz,  $t=10$  minutes
- Figure 6.10 Variation of % Gel content with treatment time for devulcanized CV system and EV system,  $f=35$  kHz,  $P=800$  W
- Figure 6.11 Variation of % Gel content with vibrating amplitude for revulcanized CV system and EV system,  $f=35$  kHz,  $t=10$  minutes
- Figure 6.12 Variation of cross-link density of devulcanized CV system with ultrasonic frequency at constant power levels (a) 50 W to 200 W (b) 500 W to 800 W,  $t=10$  minutes
- Figure 6.13 Variation of cross-link density of devulcanized CV system with treatment time at frequencies of 30, 35 and 40 kHz,  $P=800$ W
- Figure 6.14 Variation of cross-link density of devulcanized CV system with vibrating amplitude at constant ultrasonic frequencies,
- Figure 6.15 Variation of cross-link density of devulcanized CV system with ultrasonic frequency at vibrating amplitudes of 40 and 60  $\mu$ m,  $t=10$  minutes
- Figure 6.16 Variation of cross-link density of devulcanized EV system with ultrasonic frequency at constant power levels (a) 50 W to 200 W (b) 300 W to 800 W,  $t=10$  minutes
- Figure. 6.17 Variation of cross-link density of devulcanized EV system with treatment time at frequencies of 30, 35 and 40 kHz,  $P=800$ W
- Figure 6.18 Variation of cross-link density of devulcanized EV system with vibrating amplitude at constant frequencies  $t=10$  minutes

- Figure 6.19 Variation of cross-link density of devulcanized EV system with ultrasonic frequency at vibrating amplitudes of 40 and 60  $\mu\text{m}$ ,  $t=10$  minutes
- Figure 6.20 Variation of cross-link density with vibrating amplitude for devulcanized CV and EV systems,  $f=35$  kHz,  $t=10$  minutes
- Figure 6.21 Variation of cross-link density with treatment time for devulcanized CV system and EV system,  $f=35$  kHz,  $P=800$  W
- Figure 6.22 Variation of %Gel content with cross-link density for devulcanized CV system and EV system,  $f=35$  kHz,  $P=800$  W
- Figure 6.23 Cure curves of virgin and devulcanized rubber treated at 35 kHz ultrasonic frequency and at vibrating amplitudes of 78  $\mu\text{m}$  and 90  $\mu\text{m}$  (a) CV system (b) EV system
- Figure 6.24 Variation of tensile properties of revulcanized rubber, devulcanized at 35 kHz ultrasonic frequency, with vibrating amplitude (a) Tensile strength (b) Modulus @300% elongation (c) % Elongation at break

## Chapter 7

- Table 7.1 Model parameters for devulcanization model
- Table 7.2 Properties of natural rubber utilized in the simulation process
- Figure 7.1 Overstressed network fragment around an excited region
- Figure 7.2 Inflation of a cavity contained in a large body
- Figure 7.3 Variation of acoustic pressure amplitude with vibrating amplitude at the frequencies of 25,35 and 45 kHz
- Figure 7.4 Variation of acoustic pressure amplitude with ultrasonic frequency at the vibrating amplitudes of 40 and 60  $\mu\text{m}$
- Figure 7.5 Variation of interactive void concentration with vibrating amplitude at the ultrasonic frequencies of 25, 35 and 45 kHz
- Figure 7.6 Variation of interactive void concentration with ultrasonic frequency at vibrating amplitudes of 40 and 60  $\mu\text{m}$
- Figure 7.7 Variation of relative radius with time for CV system at ultrasonic frequency of 35 kHz and at amplitudes ( $\mu\text{m}$ ) of (a)4 (b)20 (c) 53 (d) 90

- Figure 7.8 Variation of relative radius with time for CV system at the frequency of 20 kHz and at amplitudes of (a) 2  $\mu\text{m}$  (b) 4  $\mu\text{m}$
- Figure 7.9 Variation of relative radius with time for CV system at the frequency of 25 kHz and at amplitudes of (a) 2  $\mu\text{m}$  (b) 4  $\mu\text{m}$
- Figure 7.10 Variation of maximum relative radius with vibrating amplitude for CV system at the frequency of 30, 35 and 40 kHz
- Figure 7.11 Variation of maximum relative radius with vibrating amplitude for CV system at the frequency of 20, 25, 45 and 50 kHz
- Figure 7.12 Variation of maximum relative radius with vibrating amplitude for CV and EV systems at the frequency of 35 kHz
- Figure 7.13 Variation of maximum relative radius with ultrasonic frequency for CV and EV systems at the vibrating amplitude of 40  $\mu\text{m}$
- Figure 7.14 Relative radius with time for CV system without considering the media response, at frequency of 35 kHz and at amplitudes of (a) 4  $\mu\text{m}$  (b) 90  $\mu\text{m}$
- Figure 7.15 Relative radius with time for CV system without considering the surface tension at the frequency of 35 kHz and at amplitudes of (a) 4  $\mu\text{m}$  (b) 90  $\mu\text{m}$
- Figure 7.16 Relative radius with time for CV system without considering the media response, at the frequency of 20 kHz and at amplitudes of (a) 2  $\mu\text{m}$  (b) 4  $\mu\text{m}$
- Figure 7.17 Variation of maximum relative radius with vibrating amplitude for CV systems at the ultrasonic frequency of 35 kHz considering with and without the media elastic response
- Figure 7.18 Variation of maximum relative radius with vibrating amplitude for CV systems at 35 kHz ultrasonic frequency, considering with and without surface tension
- Figure 7.19 Variation of different types of cross-link densities with treatment time for CV system with considered reactions that take place during devulcanization,  $f=35\text{ kHz}$ ,  $A=90\mu\text{m}$ .
- Figure 7.20 Variation of cross-link density with treatment time at constant amplitudes of (a) 4, 10, 20, 33 and 53  $\mu\text{m}$  (b) 53, 78 and 90  $\mu\text{m}$  (CV system),  $f=35\text{ kHz}$

- Figure 7.21 Variation of cross-link density with treatment time at constant amplitudes of (a) 4, 10, 20, 33 and 53  $\mu\text{m}$  (b) 53, 78 and 90  $\mu\text{m}$  (EV system),  $f=35$  kHz
- Figure 7.22 Variation of cross-link density with treatment time for CV system and EV system, at the vibrating amplitude of 90  $\mu\text{m}$  and at the ultrasonic frequency of 35 kHz
- Figure 7.23 Variation of cross-link density with vibrating amplitude for CV system and EV system, at the ultrasonic frequency of 35 kHz and at the treatment time of 10 minutes.
- Figure 7.24 Variation of cross-link density with ultrasonic frequency for (a) CV system and (b) EV system, at constant vibrating amplitudes of 40 and 60  $\mu\text{m}$  and at the treatment time of 10 minutes
- Figure 7.25 Variation of cross-link density with treatment time for (a) CV system (b) EV system at the vibrating amplitudes of 90  $\mu\text{m}$  and the ultrasonic frequency of 35 kHz
- Figure 7.26 Variation of cross-link density (theoretical and experimental values) with vibrating amplitude for (a) CV system (b) EV system at the ultrasonic frequency of 35 kHz under the treatment time of 10 minutes
- Figure 7.27 Variation of cross-link density (theoretical and experimental values) with ultrasonic frequency for (a) CV system (b) EV system at the vibrating amplitudes of 40 and 60  $\mu\text{m}$  under the treatment time of 10 minutes
- Figure 7.28 Variation of cross-link density (theoretical and experimental values) with treatment time for (a) CV system (b) EV system at the vibrating amplitudes of 90  $\mu\text{m}$  and the ultrasonic frequency of 35 kHz

## Chapter 8

Table 8.1 Additional parameters used in viscoelastic model

Figure 8.1 Relative radius versus time for one pressure cycle (a), (b) Elastic model, (c), (d) Zener model and (e), (f) Rouse model,  $f=20$  kHz

- Figure 8.2 Relative radius versus time for one pressure cycle (a), (b) Elastic model, (c), (d) Zener model and (e), (f) Rouse model,  $f=35$  kHz
- Figure 8.3 Relative radius versus time for four pressure cycles (a) Elastic model (c) Zener model and (e) Rouse model,  $f=20$  kHz,  $A=2$   $\mu\text{m}$
- Figure 8.4 Relative radius versus time for four pressure cycle (a), (b) Elastic model, (c), (d) Zener model and (e), (f) Rouse model,  $f=35$  kHz
- Figure 8.5 Relative radius versus time for ten pressure cycles for the Rouse model,  $f=35$  kHz,  $A=90$   $\mu\text{m}$

### Appendix – I

Figure A.1.1 Sigma ( $\sigma$ ) and Pi ( $\pi$ ) bonds in an ethylene molecule

Figure A.1.2 Hybrid resonance structures of polyisoprene

### Appendix – III

Figure A.3.1 Mooney-Rivlin plot for simple extension of both vulcanizing systems (symbols are experimental data and lines are fitting based on equation A.3.1)

### Appendix – V

Figure A.5.1 Apparatus for determination of total sulfur

Figure A.5.2 Apparatus for determination of sulfide sulfur

### Appendix – VI

Figure A.6.1 IR spectra of CBS accelerated sulfur vulcanized NR with CV system and with EV system



## Nomenclature

$\bar{\nabla}_{\bar{r}_0}$	A deformation gradient
$\hat{s}$	Deviatoric part of the stress tensor
$\bar{r}_0(\xi)$	Radius vector of a point in the initial configuration
$G'$	Storage modulus
$\bar{\nabla}_s \bar{r}(t)$	A relative deformation gradient
$\bar{\nabla}_r \bar{r}(s)$	A relative deformation gradient
$G''$	Loss modulus
$\bar{\nabla}_0 \bar{r}$	A deformation gradient
$\hat{\sigma}$	Cauchy stress tensor
$\bar{g}_0^i(\xi)$	Dual vector in the initial configuration
$\hat{E}_{F^*}$	Finger strain tensor
$\bar{r}(t, \xi)$	Radius vector of a point in the actual configurations
$\bar{g}^i(t, \xi)$	Dual vector in the actual configuration
$\%E_b$	Percentage elongation at break
$\chi$	Huggins interaction constant
$\rho$	Density of the material
$\mu$	Poisson's ratio
$\varphi$	Void fraction
$\sigma(\tau)$	Stress history
$\sigma(t)$	Longitudinal stress
$\epsilon(t)$	Strain at instant $t$
$\zeta_0$	Friction coefficient per monomer unit
$\Delta H$	Enthalpy difference
$\Delta L_a$	Active volume thickness
$\rho_r$	Dry density of rubber
$\tau_{Rp}$	Relaxation time for Rouse model
$\eta_s$	Viscosity of solvent
$\rho_s$	Density of solvent

$\dot{\epsilon}(t)$	Infinitesimal strain tensor
$\Delta V_a$	Active volume around a single excited region
$\tau_z$	Relaxation time for Zener model
$\Omega(t)$	A domain in the actual configuration at instant $t$
$\Omega_0$	A domain in the initial configuration
$A$	Initial cross-section area
	Vibrating amplitude
$a$	Root-mean-square end-to-end distance
$\hat{F}_*(t,s)$	Finger deformation tensor
A <sub>1</sub> S-	A sulfidic group
A <sub>2</sub> S-	A sulfidic group
$\omega$	Angular frequency
ASTM	American Society of Testing and Materials
B <sub>1</sub> S-	A sulfidic group
B <sub>2</sub> S-	A sulfidic group
$c$	Velocity of sound in rubber
C=C	Carbon-carbon double bond
$C_1$	A Mooney-Rivlin constant
$C_2$	A Mooney-Rivlin constant
CBS	N-cyclohexyl-2-benzthiazyl sulfenamide
C-C	Carbon-carbon bond
C-H	Carbon-hydrogen bond
$c_M$	Velocity defined by Mallock's formula.
$c_s$	Modified velocity of sound in rubber with voids
C-S	Carbon-sulfur bond
CV	Conventional sulfur vulcanizing system
$E$	Young's modulus
$E(t)$	Elastic modulus
$E_0$	Reference bond strength
$E_c$	Carbon-carbon bond strength
$E_i$	Bond strength of specific type of the bond
EPDM	Ethylene propylene diene terpolymer
$E_s$	Bond strength of monosulfidic cross-links

$E_{sx}$	Bond strength of polysulfidic cross-links
EV	Efficient sulfur vulcanizing system
EVA	Ethylene vinyl acetate
$f$	Force at the required elongation Ultrasonic frequency
$F$	Breaking force
$G, G(t)$	Shear modulus
$G_r$	Relaxed shear modulus
GTR	Ground tyre rubber
$G_u$	Unrelaxed modulus Shear modulus of rubber in glassy state
H	Allylic hydrogen atom
Hz	Hertz
$i$	Specific bond
$I_1$	First strain invariant
$I_2$	Second strain invariant
IPPD	N-isopropyl-N'-phenyl-p-phenylene diamine
$k$	Boltzmann constant An integer
$K_i$	A fitting parameter
$k_i$	Rate constant of the breakage of specific molecular bonds
$K_r$	A fitting parameter
$k_r$	Rate constant of the reaction of destruction of rubber bound intermediates
$k_{sl}$	Rate constant of reaction of breakage of monosulfidic cross-links
$K_{sl}$	A fitting parameter
$K_{sc}$	A fitting parameter
$k_{sc}$	Rate constant of reaction of conversion of polysulfidic cross-links to monosulfidic cross-links
$k_{sx}$	Rate constant of reaction of breakage of polysulfidic cross-links
$K_{sx}$	A fitting parameter
$K_{sxf}$	A fitting parameter
$k_{sxf}$	Rate constant of the reaction of formation of additional cross-links by reacting rubber bound intermediates with zinc complexes

$L$	Length between gauge marks at break
$L$	Large rotor
$L_0$	Initial length between gauge marks
$\xi$	Lagrangian curvilinear coordinates
$M$	Mooney viscosity number
$M_0$	Molecular weight of initial network chain
	Molecular weight of monomer unit
$M_c$	Molecular weight between cross-links
MHz	Megahertz
mm	millimeter
MPa	Megapascal
N	Newton
$n$	Number of moles of the ideal network chains
	Number of molecules per unit volume of solution
$N_0$	Initial void concentration
$N_A$	Avogadro's number
NBR	Nitrile rubber
$N_c$	Number of network chains per unit volume
$n_c$	Cross-link density
$N_c(t)$	Total concentration of cross-links remain at time $t$
$N_{cs}(t)$	Concentration of monosulfidic cross-links formed by conversion of polysulfidic cross-links to monosulfidic cross-links at time $t$
$N_i(t), N_i$	Number of specific molecular bonds per unit volume at time $t$
$N_{ia}(t)$	Active molecular bonds per unit volume at time $t$
$N_{ia}$	Number of active molecular bonds per unit volume
NMR	Nuclear magnetic resonance
NR	Natural rubber
$N_i(t)$	Concentration of rubber intermediates remaining at time $t$
$N_s(0)$	Initial concentration of monosulfidic cross-links
$N_s(t)$	Concentration of monosulfidic cross-links remaining at time $t$
$N_{sx}(0)$	Initial concentration of polysulfidic cross-links
$N_{sx}(t)$	Concentration of polysulfidic cross-links remaining at time $t$

$N_{sx}(t)$	Concentration of polysulfidic cross-links formed due to reaction of rubber bound intermediates with zinc complexes during time $t$
$N_{sxr}(t)$	Concentration of polysulfidic cross-links remains at time $t$ , after breaking into non cross-links
$N_{vk}$	Number of $k^{\text{th}}$ cross-links per unit volume
ODCB	Dissolution by o-dichlorobenzene
$P$	Power level
$p$	Sound pressure
	An integer
$P_{\infty}, P_{\infty}(t)$	Pressure at infinity in rubber
$P, P(r,t)$	Local pressure in rubber
$P_0$	Ambient pressure
$P_A$	Ultrasonic pressure amplitude
$P_c$	Critical value of the pressure difference
$P_g$	Gas pressure
phr	Parts per hundreds rubber
$P_i, P_i(t)$	Pressure in rubber at the wall.
$P_m$	Inflation pressure
$P_m(\text{elastic})$	Critical pressure for elastic model
$P_m(\text{viscoelastic})$	Critical pressure for viscoelastic model
$q$	Number of monomeric units between cross-links
$Q(t,\tau)$	Relaxation measure
$r$	Radial distance from center
$R$	Universal gas constant
$\dot{R}$	Velocity
$\ddot{R}$	Rate of change of velocity
$R(t,\tau)$	Relaxation kernel.
$R, R(t)$	Radius of a void region at time $t$
$R_0$	Initial radius of a void region
$\gamma$	Ratio of the specific heats of gas
RCOOH	An organic activator
RH	Rubber hydrocarbon
$R_{max}$	Radius of a void region at peak excitation

$R-S_{2z}-R$	Initial polysulfide cross-links
RSR	Monosulfidic cross-link
RSS	Ribbed smoke sheet
$RS_xR$	Polysulfidic cross-link
$s$	Actual configuration
$S_8$	Elementary sulfur
SBR	Styrene butadiene rubber
$\beta$	Sensitivity of void region formation
Si-C	Silicon-carbon bond
Si-O	Silicon oxygen bond
S-S	Sulfur-sulfur bond
STP	Standard test procedure
$\sigma$	Surface tension
$S_x$	Polysulfides
$t$	Treatment time
$T$	Temperature.
$T/S$	Tensile strength at break
$T_g$	Glass transition temperature
$T_{r,i}$	Radial stress on the wall due to motion
$U$	Velocity of the wall
$u$	Radial velocity in rubber relative to center
$v$	Total number of moles of various cross-links per unit volume
$V_l$	Molecular volume of the solvent
$\eta$	Viscosity of the dash pot
$v_k$	$k^{\text{th}}$ type sulfur cross-link
	Number of moles of $k^{\text{th}}$ cross-link per unit volume
$V_r$	Volume fraction of rubber in the swollen vulcanizate
$W$	Stored-energy function
W	Watt
$\lambda$	Wave length
$W_r$	Weight of dry rubber
$W_s$	Weight of solvent
$x$	An integer

X	Accelerator residue
$x(t)$	Relative radius of a void region Extension ratio
$x_3(t)$	An auxiliary function
$x_4(t)$	An auxiliary function
$X_{max}$	Relative void radius at peak excitation
$XSS_xZnS_xSX$	Zinc per-thio-salt Active sulfurating agent
$XS_xSR$	Rubber bound intermediate Accelerator-terminated polysulfidic groups Initial cross-link precursors
$XSZnSX$	Zinc accelerator complexes (zinc complexes)
y	An integer
z	An integer
ZnO	Zinc oxide
ZnS	Zinc sulfide
$\delta p$	Pressure difference
$\phi$	Velocity potential
$\mu m$	microns

